

PHARMACEUTICAL NANOTECHNOLOGY

Synthesis and Characterization of Surface-Modified PBLG Nanoparticles for Bone Targeting: *In vitro* and *In Vivo* Evaluations

İPEK ÖZCAN,¹ KAWTHAR BOUCHEMAL,² FREIMAR SEGURA-SÁNCHEZ,^{2,3} ÖZGEN ÖZER,¹ TAMER GÜNERİ,¹ GILLES PONCHEL²

¹Department of Pharmaceutical Technology, Faculty of Pharmacy, Ege University, 35100 Izmir, Turkey

²Physicochimie Pharmacotechnie Biopharmacie, Faculty of Pharmacy, Université Paris Sud-11, 92290 Chatenay-Malabry, France

³Departamento de Farmacia, Facultad de Química Farmacéutica, Universidad de Antioquia, Medellín, Colombia

Received 22 July 2010; revised 16 February 2011; accepted 3 June 2011

Published online 22 June 2011 in Wiley Online Library (wileyonlinelibrary.com). DOI 10.1002/jps.22678

ABSTRACT: In this study, poly(γ -benzyl-L-glutamate) (PBLG) polypeptide derivatives were synthesized by ring-opening polymerization of amino acid N-carboxyanhydride using selected amine-terminated initiators. Alendronate, a targeting moiety that has a strong affinity for bone, was conjugated to PBLG. Monomethoxy polyethylene glycol (PEG) was used for a hydrophilic layer on the surface of the nanoparticles (NPs) to avoid reticuloendothelial system uptake. NPs were prepared by nanoprecipitation technique not only for PBLG or PBLG–PEG but also for composite polymers with different ratios. Fluorescein isothiocyanate would be attached to the NPs as a labeling agent. The size and morphology of NPs were evaluated by dynamic laser light scattering and transmission electron microscopy, and were found to be in a useful range (less than 80 nm) for bone-targeted drug delivery. In addition, the PEGylation of NPs was supported by isothermal titration calorimetry analysis. The bone-targeting potential of NPs was evaluated *in vitro* by calcium binding and hydroxyapatite affinity assays, and *in vivo* by fluorescent imaging experiments on rats. The targeted NPs showed bright fluorescent labeling in femur tissue. These results demonstrated the possibility of optimized NPs prepared with new PBLG derivatives to accumulate in bone successfully. © 2011 Wiley-Liss, Inc. and the American Pharmacists Association *J Pharm Sci* 100:4877–4887, 2011

Keywords: poly(γ -benzyl-L-glutamate); nanoparticles; alendronate; bone targeting; PEGylation

INTRODUCTION

Targeted drug delivery is the most promising way to reduce side effects of a specific drug. In terms of “active targeting,” to deliver nanoparticles (NPs) to a desired site, site specificity is based on the affinities between targeting moiety and desired organ. The attachment of a specific moiety onto the surfaces of NPs can improve the targeting efficiency.¹ Many researchers have shown specific and efficient cellular uptake of particles that had been modified with a functional ligand with a high affinity for target cells.^{2,3}

For a successful bone targeting, the selection of targeting moieties with affinity to bone plays a key role.

When NPs reach the bone tissues, they should release the loaded drug without altering osteoblasts. The advantages of a bone-targeted drug delivery system for the treatment of bone-related diseases are obvious. Such a system could easily impart osteotropicity to a variety of bone drugs and improve their therapeutic efficacy. It is expected that the system not only increases patient comfort and compliance but also minimizes side effects of drug, especially for cancer agents. Skeletally targeted therapies have significant opportunity in the areas of osteoporosis prevention, cartilage repair, cancer treatment, fracture repair, and tissue engineering.^{4–6}

Bisphosphonates (BPs) are widely used to treat diseases characterized by osteolysis and have an exceptional affinity to hydroxyapatite (HA), the mineral phase of bone which is not present in other tissues, their rapid binding at sites of osteoclastic activity, and their ability to inhibit bone resorption.⁷ BPs

Correspondence to: İpek Özcan (Telephone: +90-232-3111368; Fax: +90-232-3885258; E-mail: ipek.ozcan@ege.edu.tr)

Journal of Pharmaceutical Sciences, Vol. 100, 4877–4887 (2011)

© 2011 Wiley-Liss, Inc. and the American Pharmacists Association

display a common backbone structure of P–C–P, where C is carbon and each P is a phosphonate group. The two-phosphonate groups are essential both for binding to HA and for the biochemical mechanism of action. This peculiarity of BPs led to explore their utility as carriers of pharmacological agents for targeting bone tissues.⁸ Among the BPs, the most important one is alendronate (ALD), which is well documented bone-targeting compound with strong bone affinity and has a primary amine useful for conjugation with our polymer.^{9,10}

Polypeptides or poly(amino acid)s are very versatile synthetic materials that fulfil many important roles in natural systems. Poly(γ -benzyl-L-glutamate) (PBLG), a synthetic polypeptide, has attracted attention for biomedical applications because of the presence of a degradable amide bond in the polymer backbone and various chemical moieties can be quite easily introduced in the structure of PBLG to form various copolymers. The functional side group of -COOH in glutamic acid units can be modified by chemical reactions to form new molecular structures of the polypeptide copolymers. Nevertheless, the peptide bonds are actually biodegraded *in vivo* by peptidases. Consequently, due to their low immunogenicity, good biocompatibility, adjustable biodegradability, and excellent mechanical properties, polypeptide-derived copolymers have drawn tremendous attention for their potential biomedical applications (carriers of drug delivery, surgical sutures, implants for bone fixation, temporary matrices, or scaffolds in tissue engineering).¹¹

Parenteral drug delivery systems based on polymeric NPs have been intensively investigated during the last decades covering a wide variety of drugs. NPs could modify the distribution of an active substance *in vivo* and increase its concentration in the target tissue, thereby improve its efficacy and reduce the toxicity.¹²

Nanoparticles are very rapidly opsonized in the bloodstream by phagocytic cells, following intravenous (i.v.) administration. To avoid the reticuloendothelial system (RES) uptake, there are two most often-mentioned criteria: the formation of a hydrophilic surface using polyethylene glycol (PEG) and obtaining particle size under 100 nm.¹³ PEGylation simply refers to the decoration of a particle surface by the covalent grafting, entrapping, or adsorbing of PEG, which is widely used for the preparation of diblock and triblock polypeptide-based copolymers as biomedical materials for its good solubility in aqueous solution, lack of toxicity, immunogenicity, and ease of excretion from living organisms.¹⁴ PEGylated nanoparticulate drug carriers made of polylactide homopolymers or poly(lactide-co-glycolide) heteropolymers copolymer with long-circulating proper-

ties present great potential for drug targeting and enhanced circulation times.¹⁵

The primary objective of our study was to synthesize novel PBLG derivatives to prepare surface-modified NPs with ALD and PEG for providing a bone-targeting drug delivery system. This study is the first report on the bone-targeting capacity of NPs prepared with these PBLG derivatives. Fluorescein isothiocyanate (FITC) was attached to the NPs as a model drug and it was confirmed visually by confocal laser scanning microscopy (CLSM). The presence of PEG onto NP surface was confirmed by isothermal titration calorimetry (ITC) experiments. The targeting capacity of NPs was also evaluated using an *in vitro* (calcium binding and HA affinity assays) and an *in vivo* (excised rat femur) approach.

MATERIALS AND METHODS

Materials

N,N-Dimethylformamide (DMF; Acros, 99%, Geel, Belgium) and benzylamine (Janssen Chimica, Beerse, Belgium) were distilled under reduced pressure over barium oxide and potassium hydroxide (KOH), respectively, and stored under argon atmosphere. γ -Benzyl-L-glutamate-N-carboxyanhydride (BLG-NCA) monomer, from ISO-CHEM-SNPE (Paris, France), was used as received. Methoxy PEG amine (mPEG-NH₂), molecular weight (MW) = 5000 g/mol from Shearwater Corporation (USA) was dried separately under vacuum over P₂O₅ at 30°C for 24 h. FITC, HA, and commercially available PBLG (PBLG-com), MW = 37,000 g/mol⁻¹ as determined by viscosity, were purchased from Sigma-Aldrich (Schnellendorf, Germany). ALD was supplied from CHEMOS GmbH (Regenstauf, Germany). α,ω -Disuccinimidyl ester PEG (Su-OOC-PEG-COO-Su), MW_{PEG} = 6000 Da, was obtained from IRIS Biotech (Marktredwitz, Germany). Purified water by reverse osmosis was used (MilliQ®; Millipore, USA). All other solvents and chemicals were of analytical grade.

Synthesis and Characterization of PBLG Derivatives

Poly(γ -benzyl-L-glutamate) derivatives (PBLG-Bnz, PBLG-PEG, and PBLG-FITC) were obtained by anionic ring-opening polymerization of BLG-NCA initiated by Bnz, mPEG-NH₂, or terminated by addition of FITC, respectively, in DMF, using a slightly modified method described in the literatures.^{16,17}

All initiator solutions were prepared under argon atmosphere and used immediately. (Bnz solution: A 0.1 mol/L solution was prepared by diluting freshly distilled benzylamine in freshly distilled DMF. mPEG-NH₂ solution: Dried mPEG-NH₂ was dissolved, at 30°C, into freshly distilled DMF to prepare

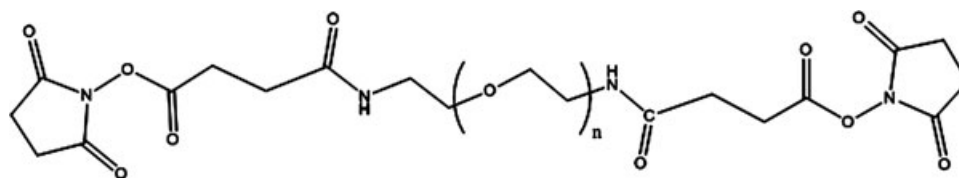


Figure 1. Structural formula of linker agent (Su-OOC-PEG-COO-Su) used for incorporation of ALD to polymer backbone.

a 0.025 mol/L solution. FITC solution: A 0.03 mol/L solution was prepared by dissolving FITC in freshly distilled DMF.)

Briefly, 32.2 mM of BLG–NCA was weighed in three-necked round-bottomed flask and dissolved in approximately 4 mL DMF (volume was adjusted to obtain a 1 mol/L solution of NCA, taking into account the volume of initiator solution needed to obtain the final initiator concentration) under mechanical stirring and argon flux at room temperature. Flask was equipped with thermometer, using refrigerant with a silica gel guard and a bubble detector. After about 10 min, the argon flux was stopped, the initiator solution (0.2 mL for Bnz solution, 0.5 mL for mPEG–NH₂ solution) was added, and CO₂ emission was observed. The reactions were conducted under argon atmosphere and mixtures were stirred at 30°C until the characteristic Fourier transform infrared (FTIR) NCA bands disappeared from spectrum (PerkinElmer 1750, USA). Furthermore, the mixture was precipitated in an excess of cold diethyl ether. The precipitates were filtered, washed with diethyl ether, and finally dried under vacuum at 35°C for at least 12 h.

For the PBLG–FITC polymers, close to the end of the PBLG–Bnz reaction, a solution containing three times more moles of FITC than initiator (Bnz) was added and after 24 h the precipitation step, described before, was made.¹⁷

First time in this study, synthesis of PBLG–PEG–ALD, which is a new PBLG derivative was described. Su–OOC–PEG–COO–Su (Fig. 1) was utilized as a linker agent to incorporate neutralized ALD to polymer. For this purpose, the agent was dissolved in 5 mL dimethyl sulfoxide (DMSO) at 2.94 mM concentration and ALD was dispersed in DMSO at 5 mM concentration. The resulting ALD mixture was slowly added to the linker agent solution drop by drop under stirring (100 rpm) during 1 h at room temperature. The mixture was allowed to react for 24 h under nitrogen atmosphere at room temperature with occasional stirring. The resulting PEG–ALD mixture was precipitated in an excess of cold diethyl ether and dried under vacuum. The synthesized PEG–ALD (15 mg) in the first step was dissolved in DMF (2 mL) and added into the finished PBLG–Bnz polymerization process after

the disappearance of NCA bands was confirmed by an FTIR spectrum. The resulting solution was kept under stirring for 24 h. Subsequently, same precipitation and drying procedures were followed as with the other PBLG derivatives. The spectroscopic characterization (¹H ³¹P NMR) was in line with the proposed structure.

To determine the average polymer molecular weights using the Mark–Houwink equation ($[\eta] = 1.58 \times 10^{-5} MW^{1.35}$), intrinsic viscosity (η) was measured at 25°C using an Ubbelohde viscometer. ¹H NMR and ³¹P NMR spectras were recorded with a Bruker Avance 400 and 200 apparatus, respectively.

Preparation of NPs

Nanoparticles were prepared from synthesized PBLG derivatives and PBLG-com by a modified nanoprecipitation method.¹⁶ Briefly, 15 mg of polymer or polymer mixture was dissolved in 5 mL of tetrahydrofuran (THF) at 30°C. This solution was added by dripping to 10 mL of MilliQ[®] (Millipore) water under magnetic stirring. The mixture was left under magnetic stirring for 15 min and transferred into a recipient vessel with a Teflon[®] surface. The solvent was evaporated, at 30°C, under a light air flow. NPs were washed with 5 mL of MilliQ[®] (Millipore) water and evaporation was carried out to yield 10 mL of NP suspension. Table 1 shows the codes and contents of the NP formulations.

Physicochemical Characterization of NPs

The mean diameter and morphology of NPs were determined by dynamic laser light scattering

Table 1. Contents of NP Formulations

Formulation Code	Polymers
F1	PBLG–Bnz
F2	PBLG–PEG
F3	PBLG–FITC
F4	PBLG–PEG–ALD
F5	PBLG-com
F6	PBLG–Bnz/PBLG–PEG (2:1)
F7	PBLG–PEG–ALD/PBLG–PEG (2:1)
F8	PBLG–Bnz/PBLG–FITC (4:1)
F9	PBLG–PEG–ALD/PBLG–FITC (4:1)
F10	PBLG–Bnz/PBLG–PEG/PBLG–FITC (2:2:1)
F11	PBLG–PEG–ALD/PBLG–PEG/PBLG–FITC (2:2:1)

(Nanosizer Coulter N4 Plus[®], UK) and transmission electron microscopy (TEM-Philips EM 208, the Netherlands). Zeta potential measurements were carried out using a Zetasizer 4, Malvern Instrument. The samples were prepared by diluting the NPs suspension with MilliQ[®] (Millipore) water. The mean value was calculated from the average of six measurements. All measurements were repeated after formulations and were kept at +4°C for 4 months to optimize storage stability conditions of the formulations.

FITC Labeling Characterization of NPs

Fluorescein isothiocyanate is a commonly used labeling agent for the *in vitro* and *in vivo* studies of micro/NP formulations.¹⁸ Jiayin and Jianmin¹⁹ reported that FITC was attached to the chitosan NPs to enable fluorescent imaging studies to be carried out. Similarly, it was thought that NPs could be prepared using FITC-labeled polymers and their targeting capacity to bone could be detected after *i.v.* injection in rats based on FITC fluorescence obtained at the bone tissue.

In this study, the fluorescent properties of NPs were investigated spectrophotometrically and microscopically. Emission spectrum was recorded with fluorescence/luminescence spectrophotometer (LS 50B; PerkinElmer, Beaconsfield, UK) at excitation 485 nm. The fluorescent image of FITC-labeled NPs was observed by CLSM (CLSM 510; ZEISS, Jena, Germany).

ITC Experiments

An isothermal calorimeter (MicroCal Inc.) with a cell volume of 1.44 mL has been used to evaluate the interactions of bovine serum albumin (BSA), a model globular protein, with PEGylated (F6 and F7) and non-PEGylated NPs (F1). The ITC instrument was periodically calibrated either electrically using an internal electric heater or chemically by measuring the dilution enthalpy of methanol in water. This standard reaction was in excellent agreement (1%–2%) with MicroCal constructor data.²⁰ In a typical experiment, aliquots of 10 μ L of BSA solution (5.4×10^{-2} mM) filled into 283 μ L syringe were used to titrate a suspension of NPs (PEGylated or non-PEGylated) (500 μ g) (2.7×10^{-2} mM) into the calorimetric cell accurately thermostated at 37°C (310 K). Intervals between injections were 300 s and agitation speed was 270 rpm. A control experiment was also performed, which consisted of successive injections of a BSA solution in the measuring cell filled with Milli-Q water. The corresponding heat flow was recorded as a function of time to account for dilution effects.

Evaluation of the Calcium-Binding Capacity and HA Affinity of Targeted NPs

The method used for the evaluation of the calcium-binding capacity was performed as described by Yalman et al.²¹ Ten microliters of standard cal-

cium solution (0.05 mEq Ca²⁺/mL) was incubated with 10 mL of NPs suspension. After incubation for 3 h under gentle magnetic stirring at 100 rpm, samples were centrifugated (MR 1812; Jouan Centrifugeurs, France) for 15 min at 3000g. Then, 1N KOH was added to supernatant to adjust the pH to 10.0. The so-prepared sample (10 mL) was mixed with ethylenediaminetetraacetic acid (EDTA) (Ca²⁺-complexing agent—0.025 M, 1 mL) and three drops of calcein solution (indicator). At this condition, samples became colored in orange-brown. The sample was then back titrated to a yellow-green end point with a standard calcium solution. The presence of magnesium improves the sharpness of the end point. With this objective, 1 mL of magnesium–EDTA complex (1:1) was added along with the titration mixture. This addition has no effect on the final determination.²² The amount of calcium bound was calculated from the difference between the initial amount of calcium added and the amount of free calcium determined in the supernatant by back titration. ALD in MilliQ[®] (Millipore) water was used as control experiment and each experiment was made in triplicate.

The HA adsorption assay was performed to evaluate the affinity of the ALD surface-modified NPs to bone.^{23,24} HA was suspended in phosphate-buffered saline (PBS) at a concentration of 10 mg·mL⁻¹. Each NP dispersion (2 mL) was mixed with HA suspension and then gently shaken for 3 h at room temperature. The sample was centrifuged at 3000g for 15 min and the supernatant solution was collected. The relative amount of NPs linked to the HA was estimated by the decrease in fluorescence intensity of these supernatant samples, in respect to the fluorescence intensity of NPs shaken with PBS and treated under the same conditions. Three replicates of each experiment were performed.

In Vivo Studies

The bone-targeting capacity of the NPs was evaluated *in vivo* using Wistar Albino rats by a protocol approved by the Ege University, Faculty of Pharmacy Animal Ethics Committee (protocol no. 2008/6-1). The animals were separated into six groups, as one saline control (Group 1) and the trial groups (Groups 2–5). Although saline solution was injected to Group 1, F8–F11-coded NPs were injected to Groups 2–5, respectively. For each experiment, six animals per group were used. NP formulations were injected to rats into the tail vein; after the injection, all animals had free access to food and water. After 24 h, animals were sacrificed by decapitation. Their femurs were isolated and processed.

Bone samples were fixed with formalin, dehydrated with acetone, embedded in poly(methyl methacrylate), and sliced with a low speed diamond saw to

the thickness of 100 μm and mounted onto a plastic cover slide for observation under a fluorescence microscope (Olympus IX71; Olympus America Corporation, Mellville, New York).

Statistical Analysis

The statistical analysis of the data was performed via analysis of variance, followed by Tukey's multiple comparisons test. A p value of less than 0.05 was considered as an evidence of a significant difference.²⁵

RESULTS AND DISCUSSION

Synthesis and Characterizations of the PBLG Derivatives

Ring-opening polymerization of α -amino acid anhydride monomers via surface attached initiator groups is the most popular and economic process for the preparation of long polypeptides. The accessibility of monomer to surface-reactive groups in this method is greater than through coupling of preformed α -helical PBLG to solid surfaces. In the coupling method, due to the strong interaction between polyglutamate molecules and many surfaces, the grafted polypeptide molecules tend to lie parallel to the surface, thus blocking other surface-binding sites and hindering subsequent chemisorption. Experimentally, in the literatures, high-molecular-weight polymers can be prepared in both good yields and large quantities by using NCA as monomer.²⁶ Similarly, the polymerization of BLG-NCA was conducted using different initiators (Bnz, mPEG-NH₂, and FITC) at 30°C under nitrogen atmosphere in our study. The results are summarized in Table 2.

Polymerizations were followed by FTIR spectroscopy. Disappearance of absorption bands at 1843, 1786, and 923 cm^{-1} corresponding to the cyclic five-

Table 2. Molecular Weights of Synthesized Polymers

Polymer	Weight Average (g/mol)	
	Theoretical ^a	Observed
PBLG-Bnz	50,000	46,300 ^b
PBLG-PEG	60,000	55,000 ^c
PBLG-PEG-ALD	60,000	70,000 ^c
PBLG-FITC	60,000	43,300 ^b

^aCalculated by considering the constitutional repeating units according to the initial ratio.

^bCalculated from viscosity measurements.

^cCalculated from ¹H NMR spectra.

ring anhydrides indicated the end of the polymerization reaction. The analysis by ¹H and ³¹P NMR (Figure 2a and 2b) confirmed the structure of the expected PBLG-PEG-ALD polymer (molar ratios of ALD/PBLG-PEG-ALD and PEG/PBLG-PEG-ALD 0.05:12 and 1:12, respectively) (CH₂PEG, 3.65; CH_{arom}, 7.26; CH₂, 5.05; CH₂, 2.56; CH, 1.74–1.85; CH, 3.74); ALD (4.94, OH; 2.51, CH₂).

The signals at 3.65 and 7.26 ppm were attributed to the PEG backbone and aromatic methylene protons of polymer in the ¹H NMR spectra, respectively. The peak at 20.42 ppm corresponds to the phosphate group of polymer in ³¹P NMR spectra.²⁷ It was confirmed that the PBLG-PEG-ALD derivatives were successfully synthesized.

Physicochemical Characterization of NPs

The homogeneous and uniform-sized NPs could be easily prepared from PBLG derivatives by modified nanoprecipitation method. Many authors showed that the nanoprecipitation technique is capable of producing stable nanoparticulate dispersions without surfactant addition.^{16,28}

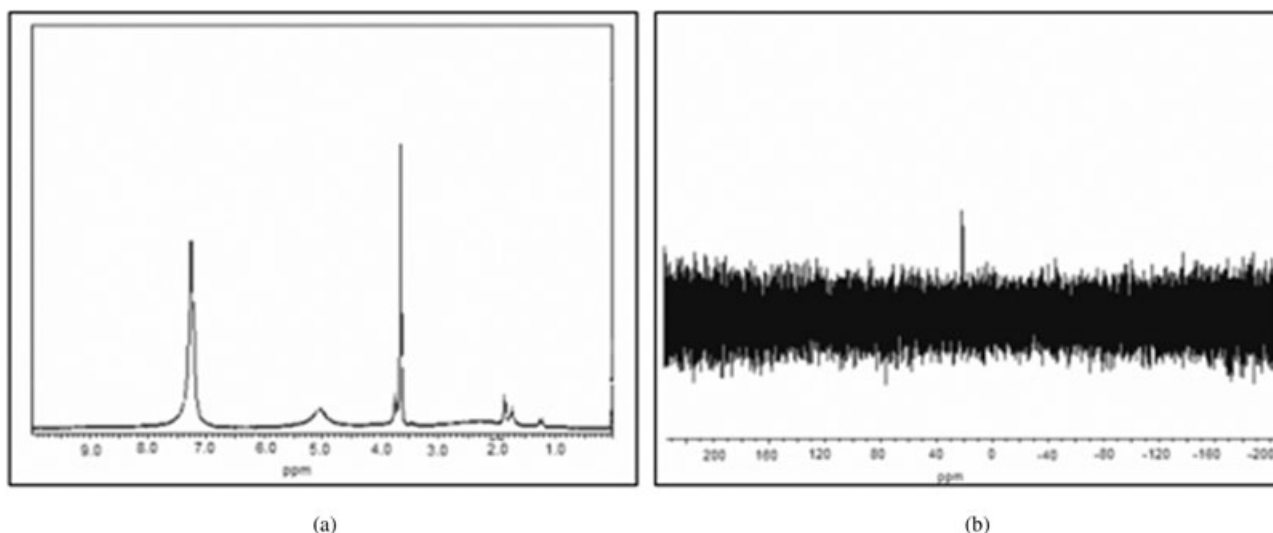


Figure 2. Spectrums of synthesized PBLG-PEG-ALD polymer: ¹H NMR (a) and ³¹P NMR (b).

Table 3. Physicochemical Characteristics of NPs Prepared with PBLG Derivatives

Formulation Code	Size (nm)	Polydispersity Index	Zeta Potential (mV)
F1	66 ± 11	0.119 ± 0.01	-30.7 ± 0.35
F2	44 ± 20	0.158 ± 0.02	-20.8 ± 0.31
F3	64 ± 15	0.122 ± 0.03	-29.8 ± 0.66
F4	71 ± 14	0.128 ± 0.02	-28.5 ± 0.80
F5	58 ± 15	0.118 ± 0.02	-29.2 ± 0.88
F6	60 ± 18	0.144 ± 0.03	-25.5 ± 0.68
F7	55 ± 14	0.137 ± 0.03	-24.8 ± 0.77
F8	65 ± 14	0.116 ± 0.03	-29.7 ± 1.33
F9	68 ± 16	0.138 ± 0.01	-28.6 ± 1.17
F10	46 ± 13	0.125 ± 0.01	-25.8 ± 1.26
F11	49 ± 15	0.118 ± 0.05	-26.5 ± 0.81

In this study, NPs prepared with PBLG derivatives were characterized in terms of size and size distribution (polydispersity index). It is evident, from the experimental data in Table 3, that the small NPs (less than 100 nm) were obtained, depending on the different polymer type and ratios of polymer mixture.

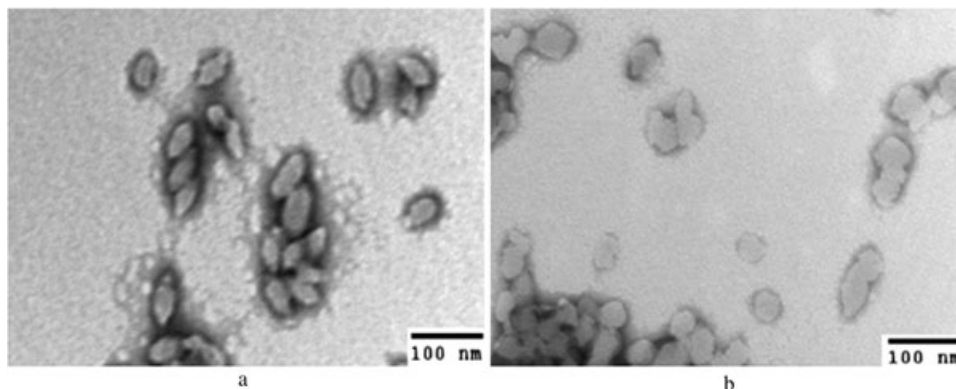
Different ratios of composite polymers were used for preliminary studies to obtain optimized NPs. And then, effective ratios were selected for NPs in terms of ideal particle size for bone-targeting applications (less than 80 nm). In the present work, we investigated the possibility to modify NP surfaces by introducing an optimal amount of a PEGylated copolymer of PBLG within the structure of NPs. Furthermore, it has been shown in a previous study that 40 wt % copolymer ratio was efficient for decreasing the activation of the complement in the plasma and avoidance from RES uptake.²⁹

The highest particle size was observed with F4-coded formulation. F1-coded NPs showed similar particle size with F3 (66 ± 11 and 64 ± 15 nm, respectively). Polymer molecular weight is one of the factors, which influence the particle size.³⁰ So, this result can be explained by the similarity in the molecular weight of the polymers used in corresponded formulations. At constant PBLG chain length, the particle size tends

to increase with increasing the chain length of PEG block, possibly due to an increase in the viscosity of the organic phase during particle preparation and to an increase of the extending PEG “brush” on the final particles. But, in our study, only one molecular weight of mPEG (5000 g/mol) was used. Therefore, differences could not be observed between NP sizes related to length of PEG. NPs were prepared from PBLG:PBLG-PEG blends, their size decreased with increasing PEG content wt % [F2(100%) < F10,F11 (33.3%) < F6,F7 (40%)], possibly because of the amphiphilic nature of these copolymers (in comparison with non-PEGylated NPs), reducing the interfacial tension between the aqueous and the organic phases. Cheng et al.³¹ reported that the NP sizes increased from 69.0 to 165.0 nm in DMF as the polymer concentration increased 10 times from 5 to 50 mg/mL. They also showed that the miscibility of the organic solvent (used to solubilize the polymer) with water could impact NP size. Our NPs prepared in THF, the most water-miscible solvent, resulted in the smallest particles, which is presumably due to more efficient solvent diffusion and polymer dispersion into water.

It is known that the dimension of vasculature pores in bone is approximately 80 nm. The hydrodynamic sizes of NPs should be less than at least 80 nm to extravasate and be localized in bone after i.v. administration. Particles larger than the local bone vasculature pores are retained in the marrow, which cause potential toxicity.^{3,32,33} The sizes of prepared NPs (F10 and F11) have a particle diameter less than 50 nm (confirmed by TEM), which is assumed to be feasible for bone-targeted drug delivery based on particles.

The calculated polydispersity index of all NP dispersions was below 0.2, indicating a narrow size volume distribution. In analogy with these results, the TEM photographs of F10- and F11-coded NPs revealed nearly ellipsoidal geometries in size around 50 nm and the NPs formed a single population (Fig. 3).

**Figure 3.** TEM micrographs of FITC-labeled targeted F10 (a) and nontargeted F11 (b) coded NPs.

The zeta potential is another important index for the characterization of the NPs. Moreover, the magnitude of the zeta potential gives an indication of the potential physical stability of a colloidal system. In general, if all the particles have a large negative or positive zeta potential, they repel each other and dispersion is considered to be stable.³⁴ In this study, all NPs have negative zeta potential because of the adsorption of anions from the aqueous polymerization medium. The zeta potential of F2-coded NPs was measured as -20.8 ± 0.31 . Non-PEGylated NPs exhibited more negative zeta potential value in comparison to PEGylated NPs. This is in agreement with other studies describing significant reductions in the zeta potential of pegylated NPs.^{35,36} However, no significant difference in zeta potential was detected between F10- and F11-coded NPs characterized by zeta potentials of -25.8 ± 1.26 and -26.5 ± 0.81 mV, respectively.

A major drawback of NP dispersions is their thermodynamic-driven tendency to lower their interfacial surface area with the environment and thus to aggregate. Because of a steric stabilization mechanism, PEGylated NPs have an increased *in vitro* stability as compared with their non-PEGylated counterparts. This mechanism can explain the ability of certain additives to inhibit coagulation of NP suspensions. These additives include certain water-loving polymers and surfactants with water-loving chains.³⁶ The presence of a hydrophilic PEG steric barrier shifts on the surface of NPs, resulting in a reduced zeta potential. In this case, F2-coded formulation prepared with PBLG-PEG polymer showed the lowest zeta potential as expected. The similar zeta potential values were observed for F6, F7, F10, and F11-coded formulations. The approximately similar ratios (33.3% and 40%) were used for these formulations. Further increase in the ratio of the PBLG-Bnz block (4:1 to 2:1) produced NPs with larger negative zeta potentials (F8-29.7; F6-25.5). This is attributed to the presence of PBLG-Bnz homopolymer in these samples.

In this study, NPs remained dispersed in a stable way in glass-capped vials at $+4^{\circ}\text{C}$ during 4 months of storage. They showed good stability of the colloidal suspension without evidence of aggregation or precipitation. This result was also confirmed by the observation of no significant changes in the particle size and zeta potential values of formulations during the course of stability study ($p > 0.05$).

Characterization of FITC-Labeled NPs

Fluorescein isothiocyanate-labeled NPs were investigated by CLSM and the particles emit green light after it was excited using a 488 nm.¹⁸ Overall, the maximal excitation and emission wavelength of formulations was found as 486 and 515 nm, respectively, by luminescence spectrophotometer. It was almost the

same as the free FITC.³⁷ The same wavelengths were found after storage of formulations during 4 months at $+4^{\circ}\text{C}$.

ITC Experiments

Isothermal titration calorimetry was used to evaluate the interactions of BSA, a model globular protein, with PEGylated and non-PEGylated NPs.³⁸ As shown in Figure 4, enthalpogram obtained with non-PEGylated NPs (F1) is different in comparison with PEGylated ones (F6 and F7). In the titration of non-PEGylated NPs, initially a series of endothermic peaks were observed subsequent to every injection. After 10 injections, a noticeable decrease in the intensity of peaks was observed and the heat flow versus time remained fairly constant. When the BSA solution was injected into a suspension of PEGylated NPs, weaker enthalpy changes were observed. These enthalpy changes were lower in the case of F7 injected.

Characterization by ITC of non-PEGylated and PEGylated NPs with BSA, a model globular protein, permitted to confirm the difference in the surface properties of two kinds of NPs. Theoretically, PEG chains grafted on NPs should avoid or, at least, reduce protein adsorption on NP surface, as a result of steric repulsions and hydrophilization. In the case of NPs composed of PBLG-PEG-ALD and PBLG-PEG, signals after each BSA injection were lower than signals observed for PBLG-Bnz and PBLG-PEG NPs. This could be explained by the presence of PEG in PBLG-PEG-ALD polymer.

Evaluation of the Calcium-Binding Capacity and HA Affinity of Targeted NPs

The calcium-binding capacity and HA affinity assay studies were determined by the titration method and fluorescence intensity measurements, respectively. In Figure 5, the amount of bound calcium was plotted against of NP formulations in the incubation medium. Binding studies were also performed with ALD in MilliQ[®] (Millipore) water.

As can be observed in Figure 5, although non-targeted PBLG NPs showed a negligible adsorption pattern, targeted PBLG NPs were able to bind calcium ions in different degrees. F11-coded formulation showed a significantly higher amount of calcium-binding capacity ($p < 0.05$) compared the F10-coded formulation. This phenomenon intimately related with the presence of ALD on the NP surface.

In the literature, NP formulations were screened *in vitro* for their bone-targeting capacity using HA powder as a model bone surface.³³ It was reported that the binding mechanism of BP to HA was simple adsorption.^{32,39} In our study, the relative fluorescent intensity was decreased in supernatant when bone-targeted F9- and F11-coded NPs were shaken with

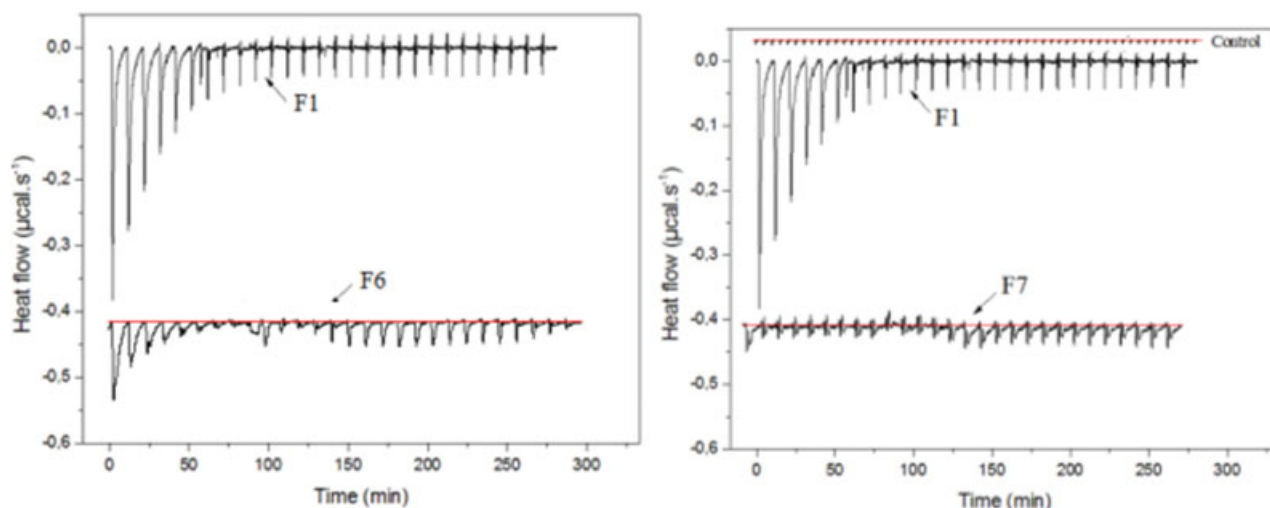


Figure 4. Typical ITC data corresponding to the titration of non-PEGylated NPs (F1) and PEGylated NPs (F6 and F7) (2.7×10^{-2} mM) with BSA solution (5.4×10^{-2} mM). Control consisted on the injection of BSA solution into MilliQ® water.

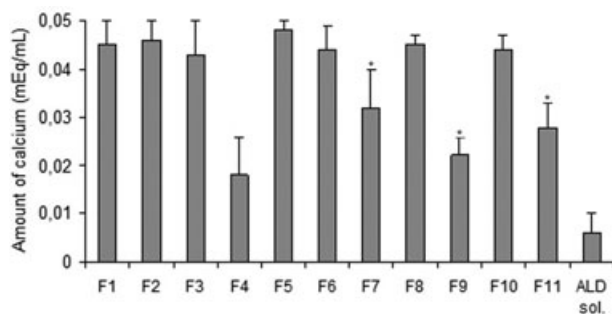


Figure 5. Amount of calcium bound onto the surface of NP formulations given in Table 1 (mean \pm SD; $n = 3$). *Statistical significance of targeted formulations (F7, F9, F11) compared with the calcium amount for their nontargeted counterparts (F6, F8, F10) is indicated. *Significantly different from nontargeted counterparts ($p < 0.05$).

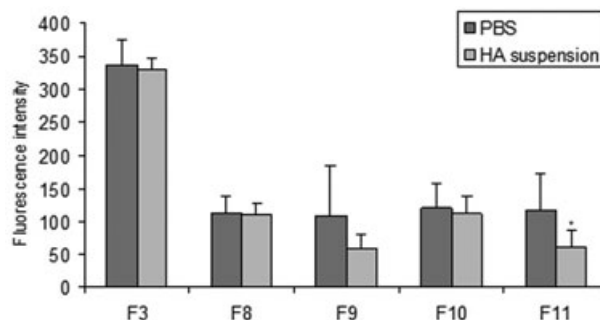


Figure 6. The fluorescence intensity of labeling formulations (F3, F8–F11) in the PBS (dark bars) and HA suspension (light bars) (mean \pm SD; $n = 3$). *Statistical significance of the fluorescence intensity of F11 formulation in PBS compared with HA suspension.

HA suspension in PBS, as can be seen in Figure 6. This result was considered to be due to the presence of ALD, which was the specific binding side of NPs to HA. On the contrary, no interaction was found between HA and F3-, F8-, F10-coded formulations as expected (see also fluorescence intensity in PBS). These results were found compatible with calcium-binding results.

In Vivo Studies

According to the previous work, the effective FITC concentration for *in vivo* imaging studies of NPs in tissues was found as 20 wt %.⁴⁰ The *in vivo* binding of the prepared NP formulations at this ratio to bone was shown in Figure 7. No autofluorescence was observed from the saline-injected animals (Fig. 7a). In those injected with nontargeted formulations (F8 and F10) (Figure 7b and 7c), negligible fluorescence label-

ing was observed when compared with targeted formulations (F9 and F11) (Figure 7d–7i). It is also noteworthy that the vasculature in bone is usually porous. Because of the small particle size (under 80 nm) of our NPs, a low accumulation could be obtained in bone tissues without a targeting moiety. In contrast, a bright fluorescence could be detected from the bones of all animals injected with FITC-labeled bone-targeting NPs (Figure 7d–7i). Moreover, F9-coded targeted NPs showed less bright fluorescence than F11-coded targeted NPs. It may be attributed to presence of the similar block length of mPEG chains on the surface of the F11-coded NPs, which can easily avoid from RES and highly reach to the bone. The presence of even an incomplete steric barrier may be sufficient to prevent interaction between PBLG–PEG NPs and phagocytic cells. This phenomenon was supported by the results of *in vivo* distribution studies on the series

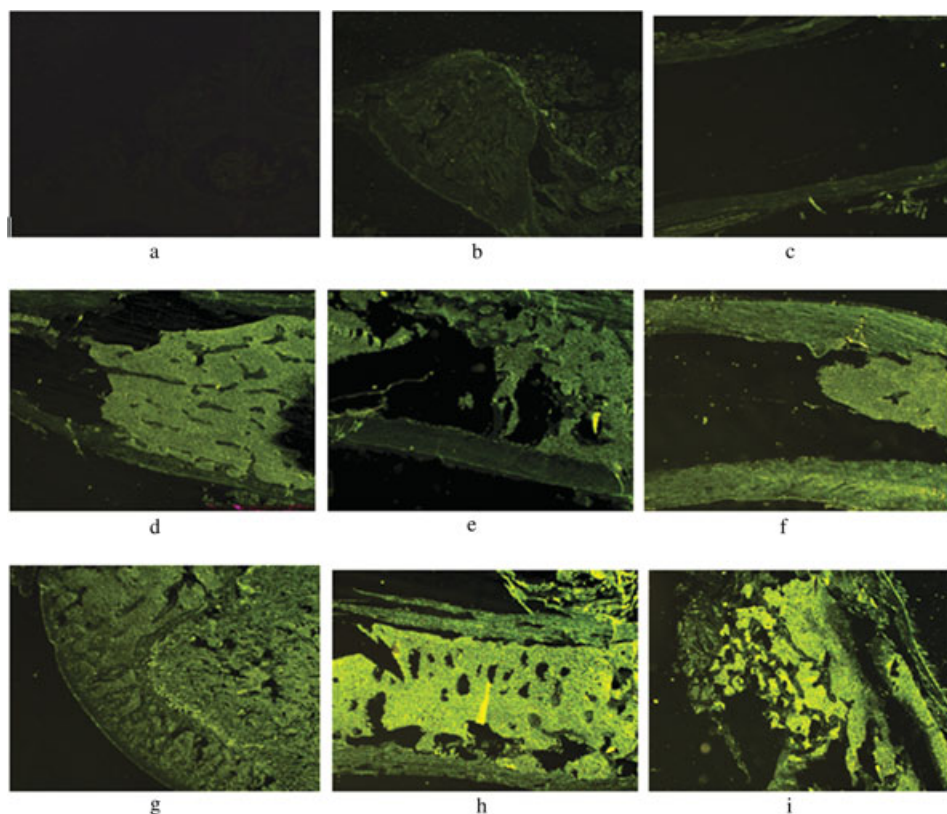


Figure 7. Histological sections of femurs: Saline injection (a). Nontargeted formulations; F8 (b) and F10 (c). Targeted formulations; F9 (d–f) (secondary spongiosa, endosteum, and periosteum of diaphyseal shaft labeled) and F11 (g–i) (epiphysis, primary and metaphyseal spongiosa, and cortex labeled).

of PBLG–PEG NPs. This is a remarkable result for the enhancement of the targeting properties of NPs.

Choi et al.³² reported that the amount of NPs adsorbed onto HA tended to be less when the large block length of mPEG. This result was due to the much longer block length of the mPEG that interfered with the potency of ALD binding to HA. The long chain length of PEG is practically helpful in the reduction of an RES response. However, its length should be optimized so as not to weaken the potency of the targeting moiety.³² In this study, one type mPEG (MW = 5000 g/mol) was used to obtain the hydrophilic PEG segment of polymers. This MW represents probably a good compromise for ensuring simultaneously optimal protein repulsion and renal excretion of the PEG segment, which is nondegradable. Furthermore, it has been shown in a more in-depth study that this copolymer was efficient for decreasing the activation of the complement in the plasma.²⁹

In our study, both the endosteum and periosteum of the diaphyseal shaft were labeled with FITC after the F9 injection (Figure 7d–7f). In addition, epiphysis, primary and metaphyseal spongiosa, and cortex of femur were marked with clear bands of FITC label after application of F11 (Figure 7g–7i). Wang

et al.³³ reported the strongest labeling around the epiphyseal–diaphyseal plates, primary spongiosa, metaphyseal spongiosa, cortex, epiphysis, endosteum, and periosteum of bone when injected in bone-targeted conjugates, not in bone marrow. Similarly, in our experiment, it was found that the fluorescent labeling in bone surface was more than that in bone marrow. It was attributed to the calcium availability in the bone structure. It appeared that the bone-targeting delivery systems preferred to accumulate in sites associated with high rates of bone turnover, perhaps in tissues where blood supplies are abundant.^{41,42}

CONCLUSIONS

The paper is concerned with the synthesis and the characterization of functional PBLG derivatives with selected molecules to further develop NP formulations for bone targeting.

Corresponding NPs were designed by surface modifications with ALD and PEG for bone-targeted drug delivery. These NPs could be prepared with convenient size for bone targeting (<80 nm) and narrow size distribution by nanoprecipitation technique. The fluorescent moiety of NPs was successfully obtained

with PBLG-FITC polymer. Moreover, no physical stability problem occurred during 4 months at +4°C. This paper also demonstrated methods to accumulate NPs onto bone surface via affinity binding between HA and ALD. *In vitro* studies confirmed the targeting capacity of these novel NP formulations. The targeting ability of these carriers to deliver a cargo to bones was reported in an animal model. All femurs of animals injected with targeted NPs showed bright fluorescence and the result supported that targeting of NPs to bones was successfully achieved. Notably, resulting PEGylated and targeted PBLG NPs demonstrated the enhanced NP delivery to bone as compared with equivalent nontargeted NPs.

Overall, the optimized nanoparticulate delivery system prepared with new PBLG derivative polymers could specifically accumulate in the bone tissue and it would be a promising candidate for bone-targeted delivery of therapeutic agents. Therefore, further investigation of this bone-targeting system is warranted.

ACKNOWLEDGMENTS

We would like to thank the European Frame Socrates/Erasmus Program for giving us the opportunity to exchange ideas and facilities in conducting this work. This study was supported by the Research Foundation of Ege University (05/ECZ/014).

REFERENCES

- Moghimi SG, Hunter AC, Murray JC. 2001. Long-circulating and target specific nanoparticles: Theory to practice. *Pharmacol Rev* 53:283–318.
- Stella B, Arpicco S, Peracchia MT, Desmaele D, Hobeke J, Renoir M, D'Angelo J, Cattel L, Couvreur P. 2000. Design of folic acid-conjugated nanoparticles for drug targeting. *J Pharm Sci* 89:1452–1464.
- Wang G, Uludag H. 2008. Recent developments in nanoparticle-based drug delivery and targeting systems with emphasis on protein-based nanoparticles. *Exp Op Drug Deliv* 5:499–515.
- Hirabayashi H, Takahashi T, Fujisaki J, Masunaga T, Sato S, Hiroi J, Tokunaga Y, Kimura S, Hata T. 2001. Bone-specific delivery and sustained release of diclofenac, a non-steroidal anti-inflammatory drug, via bisphosphonic prodrug based on the Osteotropic Drug Delivery System (ODDS). *J Control Release* 70:183–191.
- Kim K, Fisher JP. 2007. Nanoparticle technology in bone tissue engineering. *J Drug Target* 15:241–252.
- Salerno M, Cenni E, Fotia C, Avnet S, Granchi D, Castelli F, Micieli D, Pignatello R, Capulli M, Rucci N, Angelucci A, Del Fattore A, Teti A, Zini N, Giunti A, Baldini N. 2010. Bone-targeted doxorubicin-loaded nanoparticles as a tool for the treatment of skeletal metastases. *Curr Cancer Drug Targets* 10:649–659.
- Cenni E, Granchi D, Avnet S, Fotia C, Salerno M, Micieli D, Sarpietro MG, Pignatello R, Castelli F, Baldini N. 2008. Biocompatibility of poly(D,L-lactide-co-glycolide) nanoparticles conjugated with alendronate. *Biomater* 29:1400–1411.
- Hengst V, Oussoren C, Kissel T, Storm G. 2007. Bone targeting potential of bisphosphonate-targeted liposomes: Preparation, characterization and hydroxyapatite binding *in vitro*. *Int J Pharm* 331:224–227.
- Boanini E, Torricelli P, Gazzano M, Giardino R, Bigi A. 2008. Alendronate-hydroxyapatite nanocomposites and their interaction with osteoclasts and osteoblast-like cells. *Biomater* 29:790–796.
- Huang W, Wang Y, Ren L, Du C, Shi X. 2009. A novel PHBV/HA microsphere releasing system loaded with alendronate. *Mater Sci Eng C* 29:2221–2225.
- Li H, Tian Z, Wang M, Zhang A, Feng Z. 2008. Synthesis and characterization of novel triblock copolymers comprising poly(tetrahydrofuran) as a central block and poly(γ -benzyl l-glutamate)s as outer blocks. *Front Mater Sci China* 2:84–90.
- Ignjatovic NL, Liu CZ, Czernuszka JT, Uskokovic DP. 2007. Micro- and nano-injectable composite biomaterials containing calcium phosphate coated with poly(DL-lactide-co-glycolide). *Acta Biomater* 3:927–935.
- Owens DE, Peppas NA. 2006. Opsonization, biodistribution, and pharmacokinetics of polymeric nanoparticles. *Int J Pharm* 307:93–102.
- Harris JM, Chess RB. 2003. Effect of PEGylation on pharmaceuticals. *Nat Rev Drug Discov* 2:214–221.
- Wan Y, Chen W, Yang J, Bei J, Wang S. 2003. Biodegradable poly(lactide)-poly(ethylene glycol) multiblock copolymer: Synthesis and evaluation of cell affinity. *Biomater* 24:2195–2203.
- Martinez-Barbosa EM, Montebault V, Cammas-Marion S, Ponchel G, Fontaine L. 2007. Synthesis and characterization of novel poly(γ -benzyl-l-glutamate) derivatives tailored for the preparation of nanoparticles of pharmaceutical interest. *Polym Int* 56:317–324.
- Segura-Sánchez F, Montebault V, Fontaine L, Martínez-Barbosa EM, Bouchemal K, Ponchel G. 2010. Synthesis and characterization of functionalized poly(γ -benzyl-l-glutamate) derivatives and corresponding nanoparticles preparation and characterization. *Int J Pharm* 387:244–252.
- Kim TH, Park TG. 2004. Critical effect of freezing/freeze-drying on sustained release of FITC-dextran encapsulated within PLGA microspheres. *Int J Pharm* 271:207–214.
- Jiayin Z, Jianmin W. 2006. Preparation and characterization of the fluorescent chitosan nanoparticle probe. *Chin J Anal Chem* 34:1555–1559.
- Segura-Sanchez F, Bouchemal K, Lebas G, Vauthier C, Santos-Magalhaes NS, Ponchel G. 2009. Elucidation of the complexation mechanism between (+)-usnic acid and cyclodextrins studied by isothermal titration calorimetry and phase-solubility diagram experiments. *J Mol Recognit* 22:232–241.
- Yalman RG, Bruegemann W, Baker PT, Garn SM. 1959. Volumetric determination of calcium in presence of phosphate. *Anal Chem* 31:1230–1233.
- Bravo-Osuna I, Millotti G, Vauthier C, Ponchel G. 2007. *In vitro* evaluation of calcium binding capacity of chitosan and thiolated chitosan poly(isobutyl cyanoacrylate) core-shell nanoparticles. *Int J Pharm* 38:284–290.
- Bansal G, Wright JEI, Zhang S, Zernicke RF, Uludag H. 2005. Imparting mineral affinity to proteins with thiol-labile disulfide linkages. *J Biomed Mater* 74:618–628.
- Shinoda H, Adamek G, Felix R, Fleisch H, Schenk R, Hagan P. 1983. Structure-activity relationships of various bisphosphonates. *Calcif Tissue Int* 35:87–99.
- Dawson B, Trapp RG. 2001. Basic and clinical biostatistics. McGraw Hill, USA pp 161–182.
- Mori H, Iwata M, Ito S, Endo T. 2007. Ring-opening polymerization of γ -benzyl-l-glutamate-N-carboxyanhydride in ionic liquids. *Polym* 48:5867–5877.
- Casolaro M, Casolaro I, Spreafico A, Capperucci C, Frediani B, Marcolongo R, Margiotta N, Ostuni R, Mendichi R, Samperi F, Ishii T, Ito Y. 2006. Novel therapeutic agents for bone resorption. Part I. Synthesis and protonation

- thermodynamics of poly(amido-amine)s containing bisphosphate residues. *Biomacromol* 7:3417–3427.
28. Jeong YI, Seo SJ, Park IK, Lee HC, Kang IC, Akaike T, Cho CS. 2005. Cellular recognition of paclitaxel-loaded polymeric nanoparticles composed of poly(γ -benzyl l-glutamate) and poly(ethylene glycol) diblock copolymer endcapped with galactose moiety. *Int J Pharm* 296:151–161.
 29. Martinez-Barbosa E, Cammas-Marion S, Bouteiller L, Vauthier C, Ponchel G. 2009. PEGylated degradable composite nanoparticles based on mixtures of PEG-b-Poly(γ -benzyl l-glutamate) and Poly(γ -benzyl l-glutamate). *Bioconjugate Chem* 20:1490–1496.
 30. Mittal G, Sahana DK, Bhardwaj V, Ravi Kumar MNV. 2007. Estradiol loaded PLGA nanoparticles for oral administration: Effect of polymer molecular weight and copolymer composition on release behavior *in vitro* and *in vivo*. *J Control Release* 119:77–85.
 31. Cheng J, Tepy BA, Sherifi I, Sung J, Luther G, Gu FX, Levy-Nissenbaum E, Radovic-Moreno AF, Langer R, Farokhzad OC. 2007. Formulation of functionalized PLGA–PEG nanoparticles for *in vivo* targeted drug delivery. *Biomater* 28:869–887.
 32. Choi SW, Kim JH. 2007. Design of surface-modified poly(D,L-lactide-co-glycolide) nanoparticles for targeted drug delivery to bone. *J Control Release* 122:24–30.
 33. Wang D, Miller S, Sima M, Kopeckova P, Kopecek J. 2003. Synthesis and evaluation of water-soluble polymeric bone-targeted drug delivery systems. *Bioconjugate Chem* 14:853–859.
 34. Riddick TM, Ed. 2007. Control of colloid stability. In *Zeta potential*. Staunton, Virginia: Zeta-Meter Inc., pp 198–200.
 35. Yoncheva K, Lizarraga E, Irache JM. 2005. Pegylated nanoparticles based on poly(methyl vinyl ether-co-maleic anhydride): Preparation and evaluation of their bioadhesive properties. *Eur J Pharm Sci* 24:411–419.
 36. Peracchia MT, Vauthier C, Desmaele D, Gulik A, Dedieu JC, Demoy M, d'Angelo J, Couvreur P. 1998. Pegylated nanoparticles from a novel methoxypolyethylene glycol cyanoacrylate–hexadecyl cyanoacrylate amphiphilic copolymer. *Pharm Res* 15:550–556.
 37. Zhao J, Wu J. 2006. Preparation and characterization of the fluorescent chitosan nanoparticle probe. *Chin J Anal Chem* 34:1555–1559.
 38. Bouchemal K. 2008. New challenges for pharmaceutical formulations and drug delivery systems characterization using isothermal titration calorimetry. *Drug Discov Today* 13:960–972.
 39. Pan H, Sima M, Kopeckova P, Wu K, Gao S, Liu J, Wang D, Miller SC, Kopecek J. 2008. Biodistribution and pharmacokinetic studies of bone-targeting N-(2-hydroxypropyl) methacrylamide copolymer–alendronate conjugates. *Mol Pharm* 5:548–558.
 40. Ozcan I, Segura-Sanchez F, Bouchemal K, Sezak M, Ozer O, Guneri T, Ponchel G. 2010. Pegylation of poly(γ -benzyl-l-glutamate) nanoparticles is efficient for avoiding MPS capture in rats. *Int J Nanomed* 5:1103–1111.
 41. Woodard JC, Burkhardt JE, Lee W. 2002. Bones and joints. In *Handbook of toxicologic pathology*; Haschek WM, Rousseaux CG, Wallig MA, Eds. 2nd ed., Vol. 2. Academic Press: New York, pp 457–508.
 42. Zhang S, Gangal G, Uludag H. 2007. ‘Magic bullets’ for bone diseases: Progress in rational design of bone-seeking medicinal agents. *Chem Soc Rev* 36:507–531.